Author Manuscript

Author Manuscript

Author Manuscript

Author Manuscript

HHS Public Access

Author manuscript

Nat Immunol. Author manuscript; available in PMC 2012 November 01.

Published in final edited form as:

Nat Immunol. ; 13(5): 457–464. doi:10.1038/ni.2258.

Bidirectional Regulation of Neutrophil Migration by MAP Kinases

Xiaowen Liu[1,2,*], **Bo Ma**[3,*], **Asrar B. Malik**[2,7], **Haiyang Tang**[1,2], **Tao Yang**[3], **Bo Sun**[1,2,3], **Gang Wang**[1,2], **Richard D. Minshall**[2,4], **Yan Li**[5], **Yong Zhao**[3], **Richard D. Ye**[1,2,6], and **Jingsong Xu**[1,2]

[1]Department of Dermatology, University of Illinois College of Medicine, Chicago, IL.

[2]Department of Pharmacology, University of Illinois College of Medicine, Chicago, IL.

[3]State Key Laboratory of Biomembrane and Membrane Biotechnology, Institute of Zoology, Graduate School of Chinese Academy of Sciences, Beijing, China.

[4]Department of Anesthesiology, University of Illinois College of Medicine, Chicago, IL.

[5]State Key Laboratory of Brain and Cognitive Science, Institute of Biophysics, Chinese Academy of Sciences, Beijing, China.

[6]School of Pharmacy, Shanghai Jiao Tong University, Shanghai, China.

[7]The Center for Lung and Vascular Biology, University of Illinois College of Medicine, Chicago, IL.

Abstract

To kill invading bacteria, neutrophils must interpret spatial cues, migrate, and reach target sites. Although initiation of chemotactic migration has been extensively studied, little is known about its termination. Here we report that two mitogen-activated protein kinases played opposing roles in neutrophil trafficking. The extracellular signal-regulated kinase (Erk) potentiated G protein-coupled receptor kinase GRK2 activity and inhibited neutrophil migration, whereas p38 MAPK acted as a non-canonical GRK that phosphorylated the formyl peptide receptor FPR1 and facilitated neutrophil migration by blocking GRK2 function. Therefore, the dynamic balance between Erk and p38 MAPK controls neutrophil “stop” and “go” behaviors, ensuring neutrophils precisely reach their final destination as the first line of host-defense.

Introduction

Chemotaxis, or directed cell migration of cells in response to a gradient of chemoattractant is essential for lymphocytes to find antigens and for neutrophils to find sites of infection and inflammation[1]. Chemotactic cells such as blood neutrophils and neutrophil-like,

Users may view, print, copy, download and text and data- mine the content in such documents, for the purposes of academic research, subject always to the full Conditions of use: http://www.nature.com/authors/editorial_policies/license.html#terms

Correspondence should be addressed to: jingsong@uic.edu or yer@uic.edu.

*These authors contribute equally to this work.

Author contributions

X.L., B.M., Y.L., R.D.Y. and J.X. designed research; X.L., B.M., H.T., T.Y., B.S., and G.W. performed research; X.L., B.M., and J.X. analyzed data; A.B.M. R.D.M. and Y.Z. contributed new reagents and tools; X.L., B.M., A.B.M., Y.L., R.D.Y. and J.X. wrote the paper.

Author Manuscript Author Manuscript Author Manuscript Author Manuscript

differentiated HL60 cells respond to chemoattractant, such as fMet-Leu-phe (fMLP), by adopting polarized morphology (polarization) and crawling up the gradient (directional sensing). Extensive studies have been conducted to understand the mechanisms for cell polarization and directional sensing[1-4]. Neutrophils, for example, utilize a self-organizing mechanism that diverges from the same attractant receptor through different trimeric G proteins to break symmetry and polarize[5]. Both Cdc42 and microtubule pathways are important for neutrophil directional sensing[6-9]. In addition to these mechanisms that promote chemotaxis, there are inhibitory mechanisms that instruct migrating cells to stop directional movement in presence of a single attractant, and to navigate when multiple attractants are present[10]. Thus, the inhibitory mechanisms ensure chemotactic cells to reach correct destinations where they perform bactericidal functions for phagocytes and antigen identification for homing lymphocytes. To date, little is known about the regulatory mechanisms that inhibit cell migration.

Besides activating the appropriate trimeric G proteins, attractants promote phosphorylation of their receptors by G protein-coupled receptor kinases (GRKs). This phosphorylation enables the receptors to bind arrestins, which in turn prevents the receptors from activating G proteins and terminates signaling, a process termed desensitization[11-14]. The receptor-arrestin complex is subsequently internalized via either clathrin-dependent or independent pathway[14]. Internalized receptors are sorted to either degradation or recycling compartments[14]. In neutrophils, both formyl peptide receptor 1 (FPR1) internalization and decreased G protein coupling are mediated through GRK2, but do not require arrestins[12, 13]. This GRK-dependent receptor desensitization decreases the number of potential active receptors on the cell surface, thereby reducing the internal signal generated in response to a given concentration of an attractant. However, previous studies reported a negligible chemotaxis defect of cells expressing receptors that cannot be desensitized[15], suggesting receptor desensitization *per se* is not required for chemotaxis. The role of receptor desensitization in cell migration hence remains unclear.

The MAP Kinases including Erk, Jnk and p38 are involved in inflammation, apoptosis and migration[16,17]. p38 MAPK has been shown to regulate neutrophil chemotaxis both *in vivo* and *in vitro*[18-21], though the underlying mechanisms remain unclear. The roles of Erk and Jnk in chemotaxis have not been fully elucidated. Our findings indicate that the two MAPKs, p38 and Erk, differentially regulated neutrophil migration, as p38 MAPK counteracted while Erk enhanced the GRK2-mediated receptor desensitization. Furthermore, we have identified p38 MAPK as a novel G protein-coupled receptor kinase, which bound and phosphorylated FPR1. This p38-mediated phosphorylation prevented GRK2 binding to the same receptor, thus inhibiting GRK2-mediated FPR1 desensitization. Therefore, the p38 MAPK and Erk-mediated signals respectively control the net chemotactic “go” and “stop” behaviors of migrating neutrophils and enable neutrophils to arrive efficiently at the site of infection to carry out their bactericidal functions.

Author Manuscript Author Manuscript Author Manuscript Author Manuscript

Results

Opposite roles of Erk and p38 MAPK in cell migration

MAPKs have been implicated to regulate cell migration[16,17]. However, whether different MAPK isoforms play distinct roles in cell migration and the underlying mechanisms remain unclear. We treated differentiated HL60 cells with specific inhibitors for MAPKs or RNAi knockdown (**Supplementary Fig. 1**), and characterized migratory behaviors of these cells in fMLP concentration gradients generated by the EZ-taxiscan device. While ~80% of control cells (n = 109) migrated up the fMLP (100 nM) gradient and reached the top (Fig. 1a,b; Supplementary Table 1; Supplementary Video 1), only ~20% of the cells treated with RNAi for p38α (the predominant isoform expressed in HL60 cells[22]) or p38 MAPK inhibitor, SB203580 migrated through and reached the top (n = 147, Fig. 1a,b; Supplementary Table 1; Supplementary Video 2). The remaining cells were able to polarize and migrate initially in the attractant gradient, but quickly lost directionality, wandered aimlessly without net forward locomotion, thus ceasing directional migration. The chemotaxis index (CI, the ratio of net migration in correct direction to total migration length[8]) was significantly lower in p38α RNAi and SB203580-treated cells as compared to controls (0.46 and 0.41 vs. 0.72, $P < 0.001$, **Fig. 1c**). Similar results were obtained in another chemotaxis assay, in *in vivo* transmigration assay, and by using human neutrophils (**Supplementary Fig. 2,3**).

To further demonstrate the regulatory effect of p38 MAPK on cell migration, we examined migratory behaviors in p38α deficient neutrophils obtained from p38α conditional knockout mice[23]. p38α deficient neutrophils also exhibited significantly decreased transmigration *in vivo* and chemotaxis *in vitro* (**Supplementary Fig. 4a-e**), consistent with the data we observed above in SB203580 or RNAi treated cells.

In contrast to inhibiting p38 MAPK, cells treated with the Erk inhibitor, PD98059 or Erk RNAi showed increased chemotaxis compared to controls, with more than 95% cells that had migrated through the entire gradient (n = 331, Fig. 1a,b; Supplementary Table 1; Supplementary Video 3). The CI of Erk RNAi or PD98059-treated cells was significantly higher than control (0.88 and 0.92 vs. 0.72, $P < 0.001$, **Fig. 1c**). Similar results were observed with another Erk inhibitor, U0126 (**Supplementary Fig. 4**). However, inhibition of another MAPK, Jnk with SP600125 has little effects on cell migration (**Fig. 1b,c**). Cell polarization, measured by actin polymerization and cell migration speed, measured before cells lost net forward locomotion, were not affected in those p38 or Erk-inhibited cells (**Supplementary Fig. 5**; **Fig. 1d**). Thus, down-regulation of p38 MAPK inhibits directional cell migration in fMLP gradient, while inhibition of Erk enhances cell chemotaxis, suggesting that these two MAPKs have opposing functions in neutrophil chemotaxis.

Concentration-dependent cell behavioral switch

As high concentrations of chemtoattractants are known to inhibit neutrophil orientation[24], we next characterized chemotactic behaviors of differentiated HL60 cells in different fMLP concentration gradients. In gradients generated with lower concentrations of fMLP (50 and 100 nM), the majority of cells (>70%, n = 186) displayed continuous directional migration up the gradient field (**Fig. 2a,b; Supplementary Table 1**). In contrast, under higher

Author Manuscript Author Manuscript Author Manuscript Author Manuscript

concentrations of fMLP (500 nM and 1000 nM) gradient, only ~10% of cells (n = 355) completed migration through the gradient (**Fig. 2a, b; Supplementary Table 1**). The CI expectedly was significantly lower at higher fMLP concentration gradients (0.38 and 0.27 for 500 nM and 1000 nM, respectively, **Fig. 2c**) than that at lower fMLP concentration gradients (0.66 and 0.72 for 50 nM and 100 nM, respectively) (**Fig. 2c**). Similar results were obtained in neutrophil transmigration into the peritoneal cavity of wild type mice (**Fig. 2e**), using human neutrophils (**Supplementary Fig. 3**), and with cells stimulated in uniform concentrations of fMLP (used for assessment of chemokinesis, **Supplementary Fig. 2b,d**). Thus, cells migrate in response to higher concentration fMLP gradients (for example, 500 nM) exhibits a similar phenotype to cells treated with SB203580 or p38α RNAi migrating in response to lower concentration fMLP gradient (100 nM).

To address whether p38 MAPK or Erk play roles in terminating directional cell migration in above studies, we next assessed the activation of both p38 MAPK and Erk at different concentrations of fMLP. We found that activation of p38 MAPK (measured by its phosphorylation) peaked at 100 nM fMLP and severely decreased at 500 and 1000 nM fMLP (**Fig. 3a**). Activation of Erk also peaked at 100 nM fMLP but as fMLP concentration was further increased, similar amount of phosphorylated Erk was observed, indicating a plateau of Erk activation (**Fig. 3b**). In above activation assays, cells were stimulated for 2 min, as both p-p38 and p-Erk peaked at 2 min for each concentration of fMLP (**Supplementary Fig. 5c**). Similar results were obtained with human neutrophils (**Supplementary Fig. 6**).

To test whether decreased p38 MAPK activity and sustained Erk activity are responsible for impaired chemotaxis at high concentrations of fMLP, we treated cells with either a p38 MAPK activator, anisomycin (**Supplementary Fig. 1**)[25] or the Erk inhibitor, PD98059 and tested their chemotactic migration in the 500 nM gradient. Importantly, unlike most control cells that ceased directional migration in the middle of the gradient field, ~70% of p38-activated cells migrated through the field (n = 95, **Fig. 3c,d; Supplementary Table 1**). The CI thus obtained was significantly higher than control cells (0.76 vs. 0.37, P <0.001), but was comparable to the CI of control cells migrating in 100 nM fMLP gradient (**Fig. 3e,1c**). Similar results were observed when Erk was inhibited with PD98059 (**Fig. 3c-e**). The above observations indicate that p38 MAPK counteracts while Erk enhances the “stop” signal during cell chemotaxis.

MAPKs differentially regulate FPR1 internalization

We next explored the possible signal for cessation of directional cell migration induced by high concentrations of fMLP. Attractants not only activate the appropriate trimeric G proteins, but also promote receptor internalization and thus preventing receptor from activating G proteins[11-13]. We assessed whether the impaired cell migration at high concentrations of fMLP resulted from reduced receptor availability secondary to receptor internalization. We first found receptor internalization in HL60 cells or human neutrophils, measured by fluorescence-labeled fMLP, increased along with increasing fMLP concentrations (**Fig. 2f; Supplementary Fig. 6c**), consistent with a previous report[24].

Author Manuscript Author Manuscript Author Manuscript Author Manuscript

Further analysis of time response curves of the receptor internalization at 100 and 500 nM fMLP also confirmed above observations (**Supplementary Fig. 5d**).

Furthermore, to prevent receptor internalization, we used a mutant FPR1, FPR1-ΔST, in which all C-terminal Ser and Thr residues were mutated to Ala or Gly, thus the receptor cannot be internalized[15]. As expected, cells expressing wild-type FPR1 quickly arrested in a uniform concentration of 500 nM fMLP (**Fig. 4a**, top panels). The majority of cells (~70%, n = 33) lost net locomotion within the 15 min recording period (**Fig. 4b**, left panel). In contrast, only ~13% of FPR1-ΔST expressing cells (n = 69) arrested in the same recording period (**Fig. 4b**, right panel). These cells also showed negligible receptor internalization (**Fig. 4a**, bottom panels). Based on trajectories of the two groups of cells (**Fig. 4b**), the mean migration distance of the wild-type cells were significantly less than the FPR1-ΔST expressing cells (17.9 vs. 33.4 μm, $P < 0.01$, **Fig. 4c**). In conclusion, increasing concentrations of fMLP enhances receptor internalization and promotes migrating neutrophils to stop. Prevention of receptor internalization restores cell migration at high concentration fMLP, indicating that increased receptor internalization at high concentrations of chemoattractant acts as an essential “stop” signal for chemotactic neutrophils.

We next determined whether p38 MAPK and Erk have opposing effects on receptor internalization. To visualize receptor internalization, we expressed YFP-tagged FPR1 in HEK293 cells which lack endogenous FPR1. Receptor internalization became evident within 15 min after fMLP stimulation in control cells, but was seen as early as 3 min after fMLP in SB203580-treated cells (**Fig. 5a**). In contrast, much of the FPR1-YFP signal remained at the plasma membrane in PD98059-treated cells after 15 min, indicating that there was little if any receptor internalization (**Fig. 5a**). Similar results were obtained in HL60 cells (**Fig. 5b,c**) and human neutrophils (**Supplementary Fig. 6e,f**). These results collectively show that Erk and p38 MAPK differentially regulate FPR1 internalization.

GRK2 mediates the “stop” signal for chemotaxis

GRK2 is known to promote FPR1 internalization through phosphorylation[13]. To determine whether GRK2 mediates the “stop” signal during chemotaxis, we knocked down GRK2 in HL60 cells using RNAi (**Supplementary Fig. 1**), and recorded migration of these cells in the presence or absence of SB203580. As expected, inhibition of p38 MAPK reduced directional migration of control cells in the 100 nM fMLP gradient (**Fig. 6a-c; Supplementary Table 1**). Knockdown of GRK2 reversed this effect and restored cell migration (**Fig. 6a-c; Supplementary Table 1**), suggesting that SB203580-induced cell arrest was mediated through GRK2. This finding led us to test whether p38 MAPK and Erk could affect GRK2 functions. On examining membrane-associated GRK2 in control cells, we found that it was increased after fMLP stimulation (**Fig. 6d,e**). Treatment of the cells with SB203580 further increased membrane association of GRK2 at both basal and stimulated states (**Fig. 6d,e**), indicating that p38 MAPK antagonizes GRK2 membrane recruitment. Similar results were obtained in human neutrophils (**Supplementary Fig. 7**). In contrast, PD98059 prevented GRK2 membrane recruitment (**Fig. 6f,g; Supplementary Fig. 7**), suggesting that Erk enhances the effect of GRK2.

Author Manuscript Author Manuscript Author Manuscript Author Manuscript

p38 MAPK acts as a novel GRK and blocks GRK2 function

Erk has been shown to prevent GRK2 degradation[26,27]. We observed a similar effect in HL60 cells, as cells treated with Erk RNAi showed markedly decreased GRK2 protein abundance before and after fMLP stimulation (**Supplementary Fig. 8a**). However, the mechanism of how p38 MAPK regulates GRK2 remains unclear. Using immunostaining, we examined subcellular localizations of p38 MAPK and FPR1 in HL60 cells. The active p38 MAPK (p-p38) appeared in pseudopods of polarized cells; while total p38 MAPK was more uniformly distributed (**Fig. 7a**). FPR1 mainly localized to the cell membrane, at both the leading and trailing edges (**Fig. 7b**). Thus, active p38 MAPK could potentially interact with FPR1 at pseudopods. We tested this possibility using immunoprecipitation, and found increased binding of p38 MAPK to FPR1 after fMLP stimulation, which was inhibited by SB203580 (**Fig. 7c**). Similar results were also found in human neutrophils (**Supplementary Fig. 7**). In contrast, active Erk (p-Erk) was uniformly distributed and no interaction was detected between Erk and FPR1 (**Supplementary Fig. 8b,c**).

Since p38 MAPK phosphorylates Ser/Thr residues[28], and there are 19 Ser/Thr residues in the intracellular domains including 11 in the carboxyl tail of FPR1 (total 350 amino acids), we examined whether p38 MAPK phosphorylates the receptor. The three intracellular loops and the C-terminal tail of FPR1 were individually expressed as GST-tagged proteins and purified for *in vitro* phosphorylation assay. After incubation with purified active p38 MAPK, only the C-terminal tail was phosphorylated (GST-C, **Fig. 7d**); this phosphorylation was inhibited by SB203580 (data not shown). To map the phosphorylation site(s), we generated two mutants: one with the mutations of the six Ser/Thr residues within amino acids 319-332 of the C-terminal tail to Ala or Gly (MUT-A, **Fig. 7e**) and the other with the mutations of the five Ser/Thr residues among amino acids 334-342 (MUT-B, **Fig. 7e**). p38 MAPK failed to phosphorylate the MUT-B mutant (**Fig. 7d**). We next mutated each of the five Ser/Thr residues within amino acid 334-342 individually, and identified Ser342 (S342G, **Fig. 7d**) as the only phosphorylation site for p38 MAPK. Notably, the phosphorylation site for p38 MAPK (Ser342) is not the same as those for GRK2 (**Fig. 7e**), which was previously reported based on site mutagenesis[13] and shown in green color in the figure. The p38 MAPK phosphorylation site was shown in red.

We next examined whether p38 MAPK prevents GRK2 binding to FPR1. In control cells, fMLP stimulation increased binding between FPR1 and GRK2. This binding was further increased in p38 MAPK knockdown cells (**Fig. 7f**). To dissect whether phosphorylation of FPR1 by p38 MAPK prevents GRK2 binding, we constructed FLAG-tagged wild-type and two mutants of FPR1: FPR1-S342A, which prevents p38 MAPK phosphorylation; and FPR1-S342D, which mimics phosphorylation at this site. p38 MAPK bound to wild-type FPR1 and two mutants equally well (**Fig. 7g**). In contrast, GRK2 exhibited markedly decreased binding to FPR1-S342D (the phosphomimetic mutant) comparing to wild-type or FPR1-S342A (**Fig. 7g**). Furthermore, FPR1-S342D expressed HL60 cells migrated for longer distances than wild type FPR1 expressed cells in high concentration fMLP (500 nM, **Fig 7h, i**). Together, these results indicate that p38 MAPK phosphorylation at Ser342 could prevent GRK2 interaction with FPR1. Thus, p38 MAPK functions as a non-canonical G protein-coupled receptor kinase, which counteracts the function of GRK2.

Author Manuscript Author Manuscript Author Manuscript Author Manuscript

G proteins differentially regulate Erk and p38 MAPK

As shown above Erk and p38 MAPK play opposite roles in cell migration, raising the possibility that Erk and p38 MAPK antagonize each other. However, we found p38 MAPK activation was not altered in Erk RNAi cells, and *vice versa* (**Fig 8a,b**), indicating these two MAPKs are independently regulated. This contention is further supported by findings that p38 MAPK and Erk exhibit distinct activation patterns in response to increasing concentrations of fMLP (**Fig. 3; Supplementary Fig. 6**). In contrast to continuously activation of Erk, p38 MAPK displays a bell-shaped activation curve. To dissect how Erk and p38 MAPK are differentially regulated, we examined whether different heterotrimeric G proteins activated by FPR mediate Erk and p38 MAPK activation. Inactivation of Gi by pertussis toxin (PTX) abolished p38 MAPK activation, but only partially inhibited Erk activity (~70% inhibition, **Fig 8c,d**), indicating Gi-independent activation of Erk. Since Erk and p38 MAPK exhibit different activation patterns with increasing fMLP concentrations, we performed concentration dependent activation of Erk and p38 MAPK in the presence of PTX. PTX blocked p38 MAPK activation at all fMLP concentrations tested, but only partially inhibited ERK activation at each fMLP concentration (**Supplementary Fig. 9a**). To screen other possible G proteins that mediate Erk activation, we used RNAi to knock down G proteins (**Supplementary Fig. 1**). We found knocking down Gq significantly reduced fMLP induced Erk activation, but did not affect p38 MAPK activation (**Fig 8e,f**).

We further examined whether MAPK phosphatase may play a role in the differential regulation of Erk and p38 MAPK. We first tested one MAPK phosphatase, WIP1 that belongs to the protein phosphatase family 2C (PP2C) and is specific for p38 MAPK but not Erk[29]. Cells treated with okadaic acid (1nM, 30 min), a PP2 inhibitor, or RNAi knockdown of WIP1 (**Supplementary Fig. 1**), showed a delayed decline of p-p38 (**Supplementary Fig. 9**); however, neither treatment altered the bell-shaped activation curve of p38 MAPK (**Supplementary Fig. 9**). We next tested two other dual-specificity MAPK phosphatases: MKP1 and MKP5, which both de-phosphorylate Erk and p38 MAPK[30]. Knockout of either MKP1 or MKP5 increased p-p38 abundance upon stimulation with chemoattractants, but still showed a bell-shaped activation curve (unpublished observations). Thus, these phosphatases do not appear to be required for the differential activation of Erk and p38 MAPK under our experimental conditions. The possibility however still remains of differential activation of heterotrimeric G proteins by one or more FPRs, which could be responsible for the observed differences in activation of Erk and p38 MAPK.

Discussion

Understanding how chemotaxis is dynamically and precisely regulated is of great significance due to its vital roles in inflammatory cell infiltration, lymphocyte homing, embryonic development, axon guidance, and tumor invasion. In addition to triggering polarization and directional sensing which are important for initiation of neutrophil chemotaxis, chemoattractant stimulation gradually evokes a distinct stop mechanism that negatively regulates directional cell migration and brings chemotactic cells to a state similar to that of unstimulated cells. This mechanism is represented by the increment of membrane-associated GRK2 and FPR1 internalization. Our results demonstrate that, to achieve efficient

Author Manuscript Author Manuscript Author Manuscript Author Manuscript

and precise directional migration, the stop mechanism is differentially controlled by Erk and p38 MAPK. Inhibiting p38 MAPK enhances the “stop” signal and makes migrating cells arrest, while enhancing p38 MAPK or inhibiting Erk activity appears to overcome the “stop” signal and ensure directed cell migration even at high concentration of fMLP that normally induces termination of cell chemotaxis. Our results not only reveal a mechanism (Erk-GRK2) for termination of chemotaxis, but also demonstrate that sustained chemotaxis requires constant suppression (provided by p38 MAPK) of the stop mechanism before migrating cells can reach their final destinations.

Although p38 MAPK has been shown to play an important role in neutrophil chemotaxis[18-21], the underlying mechanisms are not clear. Here we demonstrate that p38 MAPK acts as a novel GRK, which phosphorylates a chemoattractant receptor and blocks the function of the classical GRK2. Different phosphorylation patterns on GPCR may instruct different signals for downstream partners to perform different functions[31]. Our observation on FPR1 supports this concept. We demonstrated that p38 MAPK and GRK2 phosphorylate the C-terminal tail of FPR1 at distinct non-overlapping sites. Phosphorylation at Ser342 of FPR1 by p38 MAPK prevents the same receptor from interacting with GRK2, thereby blocking the GRK2-mediated “stop” signals and ensuring sustained cell migration. Thus, different phosphorylation patterns on FPR1 by p38 MAPK and GRK2 execute opposite functions downstream of the receptor, indicating the subtlety of p38 regulation of neutrophil migration.

Previous studies reported negligible chemotaxis defects of cells expressing receptors that cannot be desensitized, leading to the concept that receptor desensitization is not required for chemotaxis[15]. Our findings however show that GRK2-mediated receptor internalization and desensitization play an essential role in regulating cell migration and is responsible for the termination of cell migration seen at high concentrations of attractant. Thus, it is the enhancement of receptor desensitization but not its inhibition that blocks neutrophil chemotaxis. Moreover, our findings revealed that sufficient protection of receptor against desensitization is required for sustained cell migration, and over-protection of receptor from desensitization leads to non-stop migration. Therefore to achieve precise navigation of migrating cells, it is critical to control the balance of the acceleration and deceleration of receptor desensitization, which are mediated by GRK2 and p38 MAPK, respectively. In other words, signals that control the receptor desensitization play a central role in determining the final destination of migrating neutrophils.

Our results show that different heterotrimeric G protein signals downstream of the formyl peptide receptor are responsible for the differential regulation of Erk and p38 MAPK. Activation of p38 is dependent on Gi, while both Gi and Gq signals activate Erk. In neutrophils, there are two isoforms of FPRs: FPR1 is the high affinity receptor for fMLP (Kd ~10 nM), which activates Gi; FPR2 is the low affinity receptor for fMLP (Kd ~1 μm), which also activates Gq[32]. Thus, at lower concentrations of fMLP, FPR1 activates Gi, leading to the activation of both p38 and Erk; when fMLP concentration increases, FPR2 is activated, thus activating Gq, which is responsible for sustained Erk activation. At the same time, p38 activity decreases as more FPR1 internalizes when exposed to high concentrations of fMLP. We consider that this differential regulation of two MAPKs provide bidirectional

Author Manuscript Author Manuscript Author Manuscript Author Manuscript

control on GRK2 function at different stages during directional cell migration, thus facilitating migrating cells to accurately reach their destinations.

To reach sites of infection or inflammation, circulating neutrophils must first attach to the blood vessel lining endothelial cells, then transmigrate into tissue and reach sites of infection. The mechanisms responsible for the initial arrest of neutrophils to the endothelium are predominantly mediated by β2 integrins interacting with their endothelial ligand, ICAM-1(refs. [33, 34]). Whether this initial arrest mechanism also plays a role in terminating neutrophil migration remains unclear. Likewise, it is also unknown whether MAPKs or GRKs terminate directional cell migration through regulating integrin activation. Animals such as fruit flies display concentration-dependent behavioral switch in response to odors stimulation, which is mediated by the differential regulation of neural circuits[35]. Such concentration-dependent behavioral switch can also be observed at the cellular level as a bell-shaped dose response curve during cell migration. Whereas initial increase of the concentration of an attractant leads to increased directed cell migration, it eventually peaks off and further increase of the attractant concentration causes gradual decrease of chemotaxis. Therefore studies on the cellular level may provide further molecular mechanisms and insights for understanding behavioral switch in more complex organisms. Our results suggest a model for neutrophil migration in which the dynamic balance among GRK2 and two MAPKs regulates the “go” and “stop” behaviors at the receptor level. This model provides a mechanism for concentration-dependent switch for the cell to continue its movement or stop during directional cell migration. The model of the “stop” and “go” signals as in the present study provides the opportunity for pharmacological intervention of one or more of the specific pathways. Such an intervention would enable appropriate phagocyte infiltration into inflammatory sites while minimizing neutrophil-mediated tissue injury.

Supplementary Material

Refer to Web version on PubMed Central for supplementary material.

Acknowledgement

We thank X. Du, S. Wang, B. Gantner and S. Chen for helpful discussions, and E.R. Prossnitz for providing mutant FPR1-ΔST construct. This work was supported in part by NIH grants HL095716 and AI033503, CAS grants KSCX-W-R-66 and KSCX2-YW-R-156, NSFC grants 30630037 and 31070956, and NBRP grants 2010CB945301 and 2011CB710900.

Materials and Methods

Antibodies, reagents and mice

Rabbit polyclonal antibodies against GRK2 (sc-562) and FPR1 (sc-30016), human GRK2 and Erk1/2 shRNA lentiviral particles were purchased from Santa Cruz Biotechnology. Mouse polyclonal antibodies against p38 MAPK (9228), rabbit monoclonal antibodies against phosphorylated p38 MAPK (Thr180/Tyr182, 9215) and phosphorylated p44/42 MAPK (Thr202/Tyr204, 9101) were purchased from Cell Signaling Technology. SB203580 was from Calbiochem. Human fibronectin were from BD BioSciences. Human albumin (low

Author Manuscript Author Manuscript Author Manuscript Author Manuscript

endotoxin), fMLP, C5a, protease inhibitor and phosphatase inhibitor cocktails, okadaic acid and phalloidin-TRITC were from Sigma. Fluorescein conjugate of the hexapeptide formyl-Nle-Leu-Phe-Nle-Tyr-Lys was from Invitrogen.

Wild-type C57BL/6 (WT) mice were obtained from Charles River Laboratories, *mapk14*-flox mice were obtained from Riken Bioresource Center (Japan) and B6.129 P2-Lyz2$^{tm1(cre)Ifo}$/J mice were from the Jackson Laboratory. Mice were bred and housed in pathogen-free conditions with access to food and water ad libitum in the Animal Care Facility. All experimental procedures complied with institutional and NIH guidelines for animal use.

DNA constructs and RNAi knockdown

The FPR1, p38α, and GRK2 cDNAs were cloned from RT-PCR, then inserted into pEYFP and flag-tagged vectors. FPR1-ΔST mutant was described previously[15]. GST-FPR1 loop1, loop2, loop3 were constructed by using synthesized pair wised single DNA strands and annealed pair-wise as following: 95°C for 5min, 70°C for 10min, and cool at 25°C. The fragments were inserted into eukaryotic expression plasmid pGEX-4T-2. The following sequences were used (from 5' to 3'):

LOOP1-1: GAT CCG CTG GAT TCC GGA TGA CAC ACA CAG TCA CCA CCT GAC; LOOP1-2: TCG AGT CAG GTG GTG ACT GTG TGT GTC ATC CGG AAT CCA GCG ; LOOP2-1: GAT CCG ACC GCT GTG TTT GCG TCC TGC ATC CAG TCT GGA CCC AGA ACC ACC GCA CCG TGA GCT GAC; LOOP2-2: TCG AGT CAG CTC ACG GTG CGG TGG TTC TGG GTC CAG ACT GGA TGC AGG ACG CAA ACA CAG CGG TCG; LOOP3-1: GAT CCA AGA TCC ACA AGC AAG GCT TGA TTA AGT CCA GTC GTC CCT TAC GGG TCT GAC; LOOP3-2: TCG AGT CAG ACC CGT AAG GGA CGA CTG GAC TTA ATC AAG CCT TGC TTG TGG ATC TTG.

For p38α RNAi knockdown, two pairs of sequences (#1 and #2, **Supplementary Table 2**) were used to make a shRNA expression cassette and then cloned into BamH I and Xho I restriction enzyme sites of pEN_hH1C plasmid (invitrogen). By using the LR recombination reaction, shRNA expression cassette was inserted into lentiviral shRNA expression plasmid pDSL_hpUGIP, then co –transfected with pspAX2 and pMD2.G into 293FT cell line to package lentivirus particles. Suspension was harvested 72 hours after transfection and used to infected HL60 cells. Puromycin was used to screen the stable p38α RNAi cell line.

For GRK2, Erk1/2, G12, G13, Gq, and WIP1 RNAi knockdown, the lentiviruses were purchased from Santa Cruz Biotechnology. The sequences of siRNA of each proteins are listed in supplementary table 2.

Cell culture, transfection and isolation of human neutrophils

Procedures for cultivation and differentiation of HL-60 have been described[5]. For transient transfections, differentiated HL-60 cells (on day 6 after addition of DMSO) were washed once in RPMI-HEPES and resuspended in the same medium to a final concentration of 10^8 ml^{-1}. DNA was then added to the cells (30 μg of FPR1-YFP or FPR1-ΔST-YFP DNA), the

Author Manuscript Author Manuscript Author Manuscript Author Manuscript

cell-DNA mixture was incubated for 10 min at 25°C , transferred to electroporation cuvettes and subjected to an electroporation pulse on ice at 310 V, 1180 μF and low resistance. Transfected cells were allowed to recover for 10 min at 25°C and then transferred to 20 ml complete medium. Subsequent assays were performed 4-6 h after transfection.

For isolation of human neutrophils, blood was collected from healthy human donors. Erythrocytes were removed using dextran sedimentation (4.5% dextran) followed by hypotonic lysis using distilled water. Neutrophils were isolated from the resulting cell suspension using discontinuous Percol gradient centrifugation. This procedure yielded >95% neutrophil purity and >95% viability as assessed by flow cytometry. Studies using human neutrophils were approved by the Institutional Review Board of University of Illinois at Chicago.

Cell migration assays

Live cells were imaged after stimulation either with a uniform concentration of fMLP or a concentration gradient generated by *EZ-taxiscan*™ device or micropipette. For EZ-taxiscan assay, cells migrated over a 50 μg/ml fibronectin coated cover glass on a horizontal glass surface under a silicon chip. dHL60 cells were pretreated with or without the inhibitors, p38 inhibitor SB203580 (10μM), Erk1/2 inhibitor PD98059 (50μM), Jnk inhibitor SP600925 (10μM), or MAPK activator anisomycin (1μM) for 30min, then washed with RPMI/25mM HEPES/0.1% BSA and resuspended in RPMI/25mM HEPES/0.1% BSA solution. Cells were loaded to the bottom of the chip, and chemoattractant was added to the top of the chip to generate a chemoattractant gradient. Cells migrated for 30 min and images were recorded with the EZ-taxiscan software and then analyzed in Image J.

For micropipette assay, the gradient was generated by a point source of chemoattractant from a micropipette containing 10 μM fMLP. Time-lapse video microscopy was performed as described[5]. The cell migratory behaviors were recorded and analyzed in Image J.

For neutrophil peritoneal transmigration, mice were injected with saline (100 μl), different doses of fMLP (1, 10, 100, 1000nM in 100 μl saline, ip.). After 4 h, peritoneal cavities of anesthetized mice were lavaged, and leukocytes were recovered. The total number of leukocytes was counted using a hemocytometer and neutrophil counts were determined on 100 μl cytospins stained with Diff-Quik and presented as percent total population.

Immunoprecipitation and immunofluorescence

Immunoprecipitation and immunofluorescence were performed as described[36]. Densitometry of bands on autoradiogram was performed with scanned x-ray films and the Image J program. Results of at least 3 independent experiments are represented as a bar graph using arbitrary units to compare the intensity of the bands.

Phosphorylation assay of p38 MAPK in vitro

To start the reaction, active p38α MPAK (40 ng/μl) was incubated with the substrate, FPR1-C in 1× assay buffer together with 250μM ATP, 0.16μCi/μl ^{32}p-γATP. After 15 minutes,

Author Manuscript Author Manuscript Author Manuscript Author Manuscript

reaction was terminated by adding 25μl 2× sample buffer and boiled for 10 minutes, and subjected to SDS-PAGE and read with Fijifilm Fluorescent and Radioisotope Science Imaging Systems FLA-7000.

fMLP surface binding assay

dHL60 cells were pretreated with or without 10 μM SB203580 or 50 μM PD98059 for 30min at 37°C, then washed with RPMI 1640 and HBSS. Cells were resuspended in HBSS and then simulated with fMLP for indicated times, and the reaction was quenched with the addition of 10 volumes of ice-cold HBSS buffer. The cells were then washed extensively and incubated with 10 μM *N*-formyl-Nleu-Leu-Phe-Nleu-Tyr-Lys-fluorescein prior to analysis by flow cytometry. Unlabeled 10 μM fMLP stimulated cells were used as a negative control.

Membrane bound GRK2 assay

dHL60 cells were pre-incubated in RPMI 1640 with or without inhibitors (SB203580, 10 μM or PD98059, 50 μM) for 30 min in suspension. Cells were then harvested and suspended in modified Hanks' balanced salt solution (HBSS) (10^7 cells in 0.5 ml), and stimulated for indicated time with 100 nM fMLP in suspension. Simulation was stopped by the addition of 0.5 ml of stopping buffer at 25°C (100 mM Mes, pH 6.8/5 mM EDTA/10 mM $MgCl_2$/1% Triton X-100/1× Protease Inhibitor Mixture). Samples were incubated at 25°C for 15 min and then centrifuged for 5 min at 15,000 g and 25°C. Pellets were resuspended in 2× laemmli buffer and boiled for 10 min for SDS-PAGE. After transferred to PVDF membrane, mouse anti-GRK2 monoclonal antibody (sc-13143) was used to detect the membrane bounded GRK2. GRK2 and GAPDH in supernatant were also examined.

Statistical analysis

Statistical comparisons were made using two-tailed Student's *t* test. Experimental values are reported as the mean ± SEM. Differences in mean values were considered significant at $P < 0.05$.

References

1. Devreotes PN, Zigmond SH. Chemotaxis in eukaryotic cells: a focus on leukocytes and Dictyostelium. Annu Rev Cell Biol. 1988; 4:649–686. [PubMed: 2848555]
2. Ridley AJ, et al. Cell migration: integrating signals from front to back. Science. 2003; 302:1704–1709. [PubMed: 14657486]
3. Swaney KF, Huang CH, Devreotes PN. Eukaryotic chemotaxis: a network of signaling pathways controls motility, directional sensing, and polarity. Annu Rev Biophys. 2010; 39:265–289. [PubMed: 20192768]
4. Janetopoulos C, Firtel RA. Directional sensing during chemotaxis. FEBS Lett. 2008; 582:2075–2085. [PubMed: 18452713]
5. Xu J, et al. Divergent signals and cytoskeletal assemblies regulate self-organizing polarity in neutrophils. Cell. 2003; 114:201–214. [PubMed: 12887922]
6. Srinivasan S, et al. Rac and Cdc42 play distinct roles in regulating PI(3,4,5)P3 and polarity during neutrophil chemotaxis. J. Cell Biol. 2003; 160:375–385. [PubMed: 12551955]

Author Manuscript Author Manuscript Author Manuscript Author Manuscript

7. Li Z, et al. Directional sensing requires G beta gamma-mediated PAK1 and PIX alpha-dependent activation of Cdc42. Cell. 2003; 114:215–227. [PubMed: 12887923]
8. Xu J, Wang F, Van Keymeulen A, Rentel M, Bourne HR. Neutrophil microtubules suppress polarity and enhance directional migration. Proc Natl Acad Sci USA. 2005; 102:6884–6889. [PubMed: 15860582]
9. Xu J, et al. Polarity reveals intrinsic cell chirality. Proc Natl Acad Sci USA. 2007; 104:9296–9300. [PubMed: 17517645]
10. Foxman EF, Campbell JJ, Butcher EC. Multistep navigation and the combinatorial control of leukocyte chemotaxis. J. Cell Biol. 1997; 139:1349–1360. [PubMed: 9382879]
11. Lefkowitz RJ. G protein-coupled receptors. III. New roles for receptor kinases and beta-arrestins in receptor signaling and desensitization. J. Biol. Chem. 1998; 273:18677–18680. [PubMed: 9668034]
12. McLeish KR, Gierschik P, Jakobs KH. Desensitization uncouples the formyl peptide receptor-guanine nucleotide-binding protein interaction in HL60 cells. Mol. Pharmacol. 1989; 36:384–390. [PubMed: 2506429]
13. Prossnitz ER, Kim CM, Benovic JL, Ye RD. Phosphorylation of the N-formyl peptide receptor carboxyl terminus by the G protein-coupled receptor kinase, GRK2. J. Biol. Chem. 1995; 270:1130–1137. [PubMed: 7836371]
14. Moore CA, Milano SK, Benovic JL. Regulation of receptor trafficking by GRKs and arrestins. Annu Rev Physiol. 2007; 69:451–482. [PubMed: 17037978]
15. Hsu MH, Chiang SC, Ye RD, Prossnitz ER. Phosphorylation of the N-formyl peptide receptor is required for receptor internalization but not chemotaxis. J. Biol. Chem. 1997; 272:29426–29429. [PubMed: 9367998]
16. Johnson GL, Lapadat R. Mitogen-activated protein kinase pathways mediated by ERK, JNK, and p38 protein kinases. Science. 2002; 298:1911–1912. [PubMed: 12471242]
17. Huang C, Jacobson K, Schaller MD. MAP kinases and cell migration. J. Cell Sci. 2004; 117:4619–4628. [PubMed: 15371522]
18. Nick JA, et al. Common and distinct intracellular signaling pathways in human neutrophils utilized by platelet activating factor and FMLP. J Clin Invest. 1997; 99:975–986. [PubMed: 9062356]
19. Cara DC, Kaur J, Forster M, McCafferty DM, Kubes P. Role of p38 mitogen-activated protein kinase in chemokine-induced emigration and chemotaxis in vivo. J Immunol. 2001; 167:6552–6558. [PubMed: 11714824]
20. Heit B, Tavener S, Raharjo E, Kubes P. An intracellular signaling hierarchy determines direction of migration in opposing chemotactic gradients. J. Cell Biol. 2002; 159:91–102. [PubMed: 12370241]
21. Zu YL, et al. p38 mitogen-activated protein kinase activation is required for human neutrophil function triggered by TNF-alpha or FMLP stimulation. J Immunol. 1998; 160:1982–1989. [PubMed: 9469462]
22. Hale KK, Trollinger D, Rihanek M, Manthey CL. Differential expression and activation of p38 mitogen-activated protein kinase alpha, beta, gamma, and delta in inflammatory cell lineages. J Immunol. 1999; 162:4246–4252. [PubMed: 10201954]
23. Nishida K, et al. p38alpha mitogen-activated protein kinase plays a critical role in cardiomyocyte survival but not in cardiac hypertrophic growth in response to pressure overload. Mol Cell Biol. 2004; 24:10611–10620. [PubMed: 15572667]
24. Sullivan SJ, Zigmond SH. Chemotactic peptide receptor modulation in polymorphonuclear leukocytes. J. Cell Biol. 1980; 85:703–711. [PubMed: 7391138]
25. Barros LF, Young M, Saklatvala J, Baldwin SA. Evidence of two mechanisms for the activation of the glucose transporter GLUT1 by anisomycin: p38(MAP kinase) activation and protein synthesis inhibition in mammalian cells. J Physiol. 1997; 504(Pt 3):517–525. [PubMed: 9401960]
26. Theilade J, Hansen JL, Haunso S, Sheikh SP. MAP kinase protects G protein-coupled receptor kinase 2 from proteasomal degradation. Biochem. Biophys. Res. Comm. 2005; 330:685–689. [PubMed: 15809051]

Author Manuscript Author Manuscript Author Manuscript Author Manuscript

27. Theilade J, Lerche Hansen J, Haunso S, Sheikh SP. Extracellular signal-regulated kinases control expression of G protein-coupled receptor kinase 2 (GRK2). FEBS Lett. 2002; 518:195–199. [PubMed: 11997045]
28. Ono K, Han J. The p38 signal transduction pathway: activation and function. Cell. Signal. 2000; 12:1–13. [PubMed: 10676842]
29. Takekawa M, et al. p53-inducible wip1 phosphatase mediates a negative feedback regulation of p38 MAPK-p53 signaling in response to UV radiation. EMBO J. 2000; 19:6517–6526. [PubMed: 11101524]
30. Dickinson RJ, Keyse SM. Diverse physiological functions for dual-specificity MAP kinase phosphatases. J. Cell Sci. 2006; 119:4607–4615. [PubMed: 17093265]
31. Zidar DA, Violin JD, Whalen EJ, Lefkowitz RJ. Selective engagement of G protein coupled receptor kinases (GRKs) encodes distinct functions of biased ligands. Proc Natl Acad Sci USA. 2009; 106:9649–9654. [PubMed: 19497875]
32. Ye RD, et al. International Union of Basic and Clinical Pharmacology. LXXIII. Nomenclature for the formyl peptide receptor (FPR) family. Pharmacol. Rev. 2009; 61:119–161. [PubMed: 19498085]
33. Butcher EC. Leukocyte-endothelial cell recognition: three (or more) steps to specificity and diversity. Cell. 1991; 67:1033–1036. [PubMed: 1760836]
34. Springer TA. Traffic signals for lymphocyte recirculation and leukocyte emigration: the multistep paradigm. Cell. 1994; 76:301–314. [PubMed: 7507411]
35. Semmelhack JL, Wang JW. Select Drosophila glomeruli mediate innate olfactory attraction and aversion. Nature. 2009; 459:218–223. [PubMed: 19396157]
36. Xu J, et al. Nonmuscle myosin light-chain kinase mediates neutrophil transmigration in sepsis-induced lung inflammation by activating beta2 integrins. Nat. Immunol. 2008; 9:880–886. [PubMed: 18587400]

Author Manuscript Author Manuscript Author Manuscript Author Manuscript

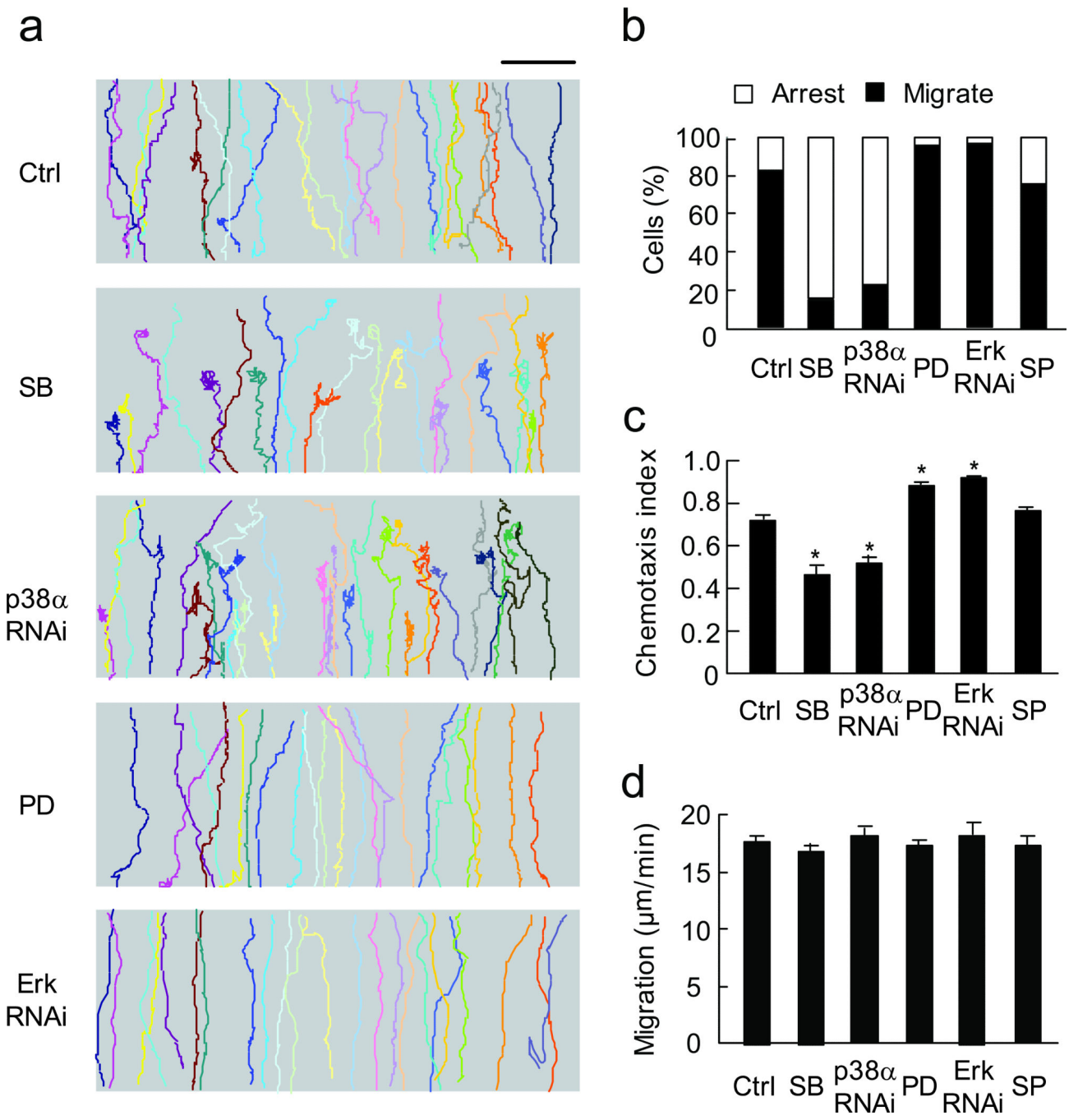

Figure 1. Erk and p38 MAPK play opposite roles in neutrophil chemotaxis

(**a**) Trajectories of control (Ctrl), SB203580 (SB, 10 μM), p38 RNAi, PD98059 (PD, 50 μM) and Erk RNAi-treated cells in 100 nM fMLP gradient. Each trace represents one individual cell trajectory. Three independent experiments were performed, each using > 30 cells per condition, one of representative experiments is shown. Bar, 100 μm. (**b**) Relative percentage of cells migrated through the entire gradient field (black bars) compared to cells failed to reach the top (open bars) in above five groups and SP600125 (SP, Jnk inhibitor at 10 μM)-treated cells. (**c**) Chemotaxis index (CI) of above six groups of cells. *, $P < 0.001$, compared

Author Manuscript Author Manuscript Author Manuscript Author Manuscript

to control, bars indicate mean ± SEM. (**d**) Migration speed of the six groups of cells. Bars indicate mean ± SEM.

Author Manuscript Author Manuscript Author Manuscript Author Manuscript

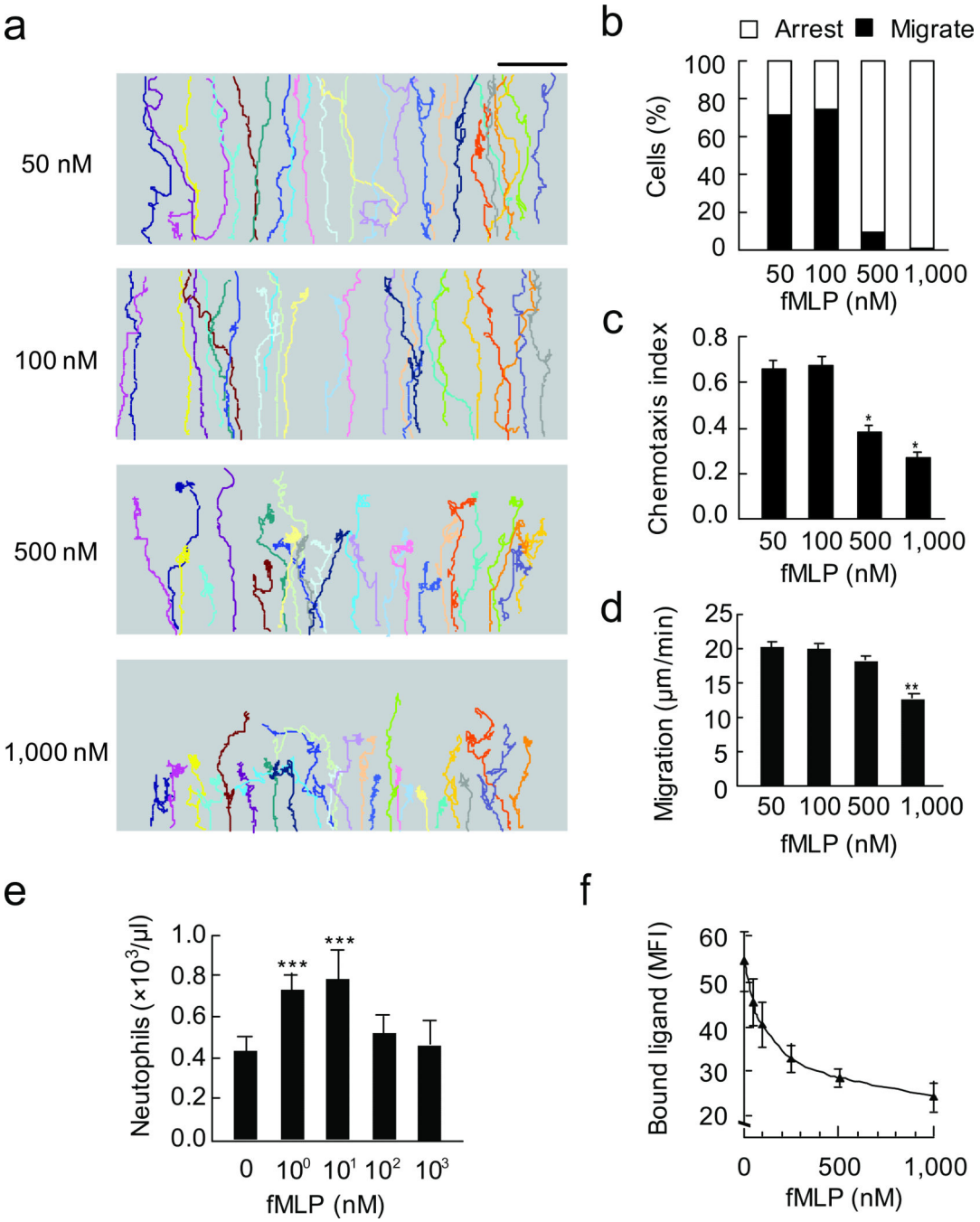

Figure 2. Concentration-dependent behavioral switch for neutrophil chemotaxis and transmigration

(**a**) Cell trajectories in four different fMLP concentration gradients generated by the EZ-taxiscan device. Each trace represents one individual cell trajectory. Three independent experiments were performed, each using > 30 cells per condition, one of representative experiments is shown. Bar, 100 μm. (**b**) Relative percentage of cells migrated through (black bars) compared to cells arrested (open bars) in four groups described above. (**c**) CI of the four groups of cells. *, $P < 0.001$ compared to CI at 100 nM fMLP, bars indicate mean ±

Author Manuscript Author Manuscript Author Manuscript Author Manuscript

SEM. (**d**) Migration speed of the four groups of cells. **, $P < 0.001$ compared to speed at 100 nM fMLP, bars indicate mean ± SEM. (**e**) Neutrophil emigration into the peritoneal cavity in response to injection of different concentrations of fMLP. For all groups, n = three to four mice. One of three separate experiments is shown. ***, $P < 0.05$ compared to basal. (**f**) Receptor internalization at different concentration of fMLP, shown as mean fluorescence intensity of bound ligand. Results indicate mean ± SEM.

Author Manuscript Author Manuscript Author Manuscript Author Manuscript

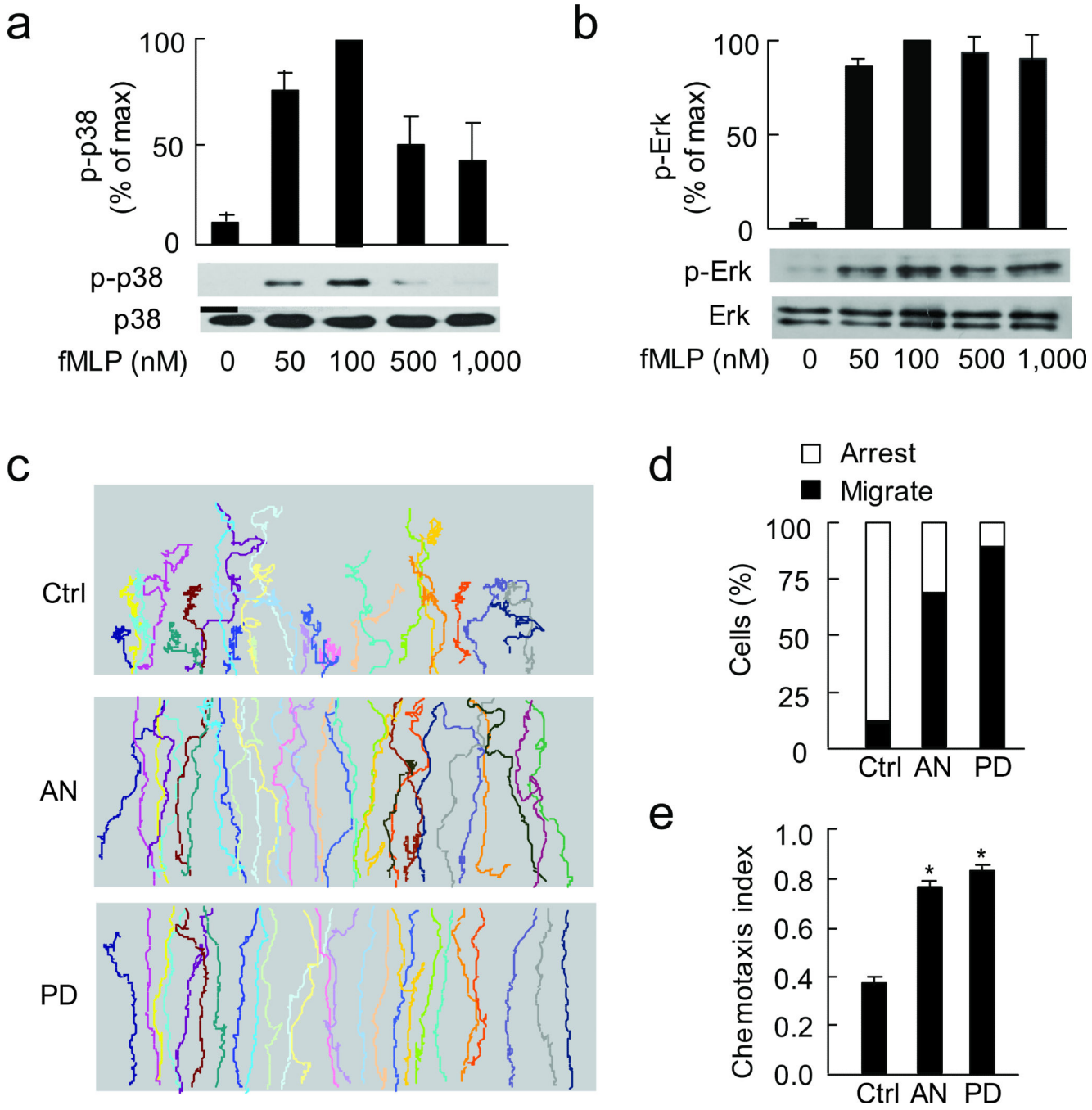

Figure 3. Inhibition of Erk or enhancement of p38 MAPK restores cell migration at high concentration of fMLP

(**a, b**) Immunoblots show p-p38, p38 (**a**), p-Erk and Erk (**b**) at different concentrations of fMLP (stimulated for 2 min). p-p38 and p-Erk values were compared to the maximum activation at 100 nM fMLP (as 100). *N* = 3, one of representative experiments is shown; bars indicate mean ± SEM. (**c**) Trajectories of control, anisomycin (AN, 1 μM) and PD98059 (PD, 50 μM)-treated cells in 500 nM fMLP gradient. Three independent experiments were performed, each using > 30 cells per condition, one of representative experiments is shown. (**d**) Relative percentage of cells migrated through (black bars) compared to cells arrested

Author Manuscript Author Manuscript Author Manuscript Author Manuscript

(open bars) in three groups described above. (**e**) CI of the three groups of cells. *, $P < 0.001$ compared to control. Results are mean of 3 independent experiments; bars indicate mean ± SEM.

Author Manuscript Author Manuscript Author Manuscript Author Manuscript

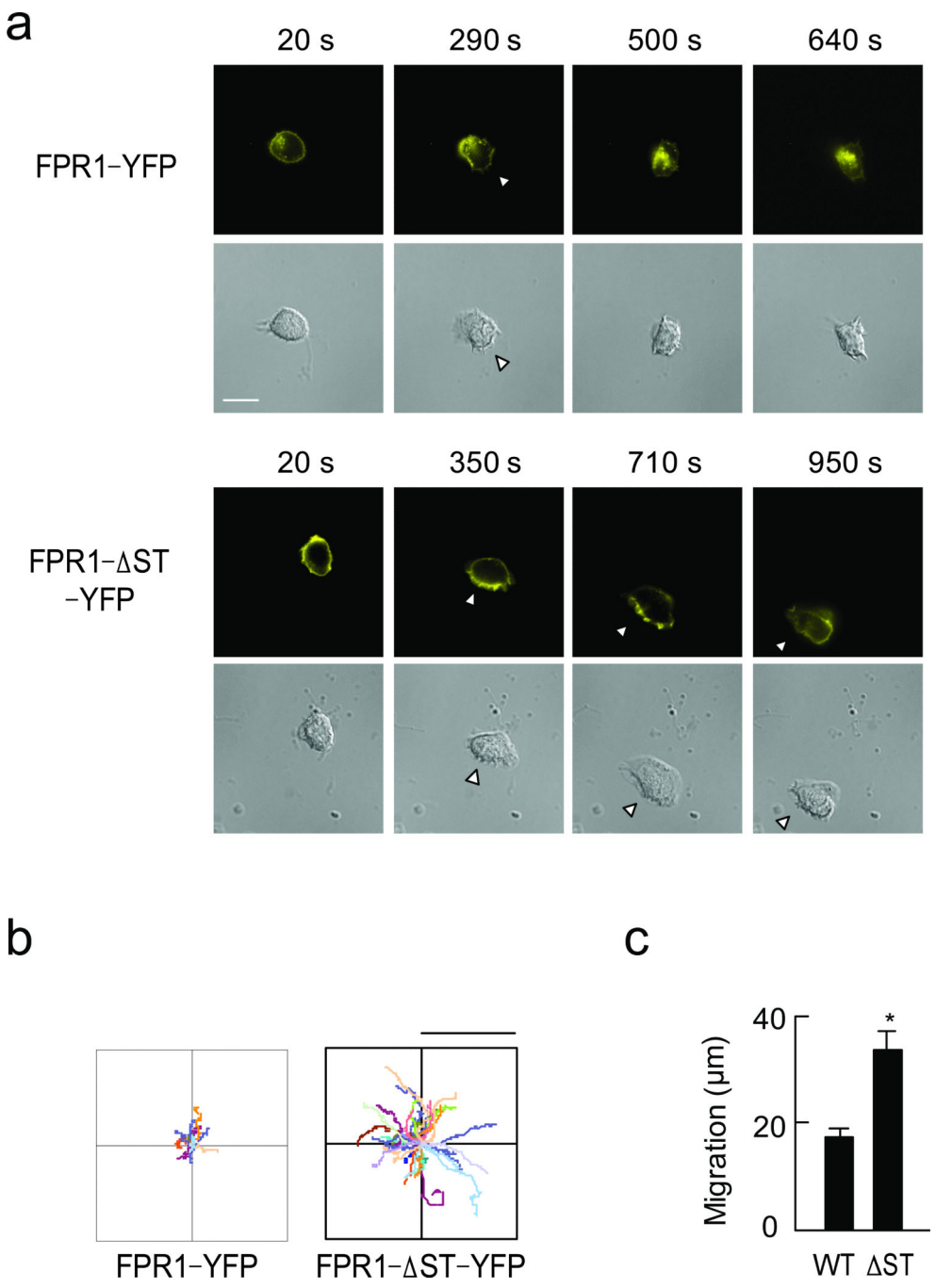

Figure 4. Receptor internalization acts as a "stop" signal for directional migration

(**a**) Fluorescence and Nomarski images of FPR1-YFP and FPR1-ΔST-YFP expressing cells stimulated with fMLP (500 nM) for indicated times. Arrowheads point to the leading edges. $N > 30$ cells of each group, one representative cell of each group is shown. Bar, 10 μm. (**b**) Trajectories of FPR1-YFP and FPR1-ΔST-YFP expressing cells stimulated with fMLP (500 nM). Three independent experiments were performed, each using > 30 cells per condition. Bar, 60 μm. (**c**) Distance migrated of above two groups of cells. *, $P < 0.01$. Results are mean of 3 independent experiments; bars indicate mean ± SEM.

Author Manuscript Author Manuscript Author Manuscript Author Manuscript

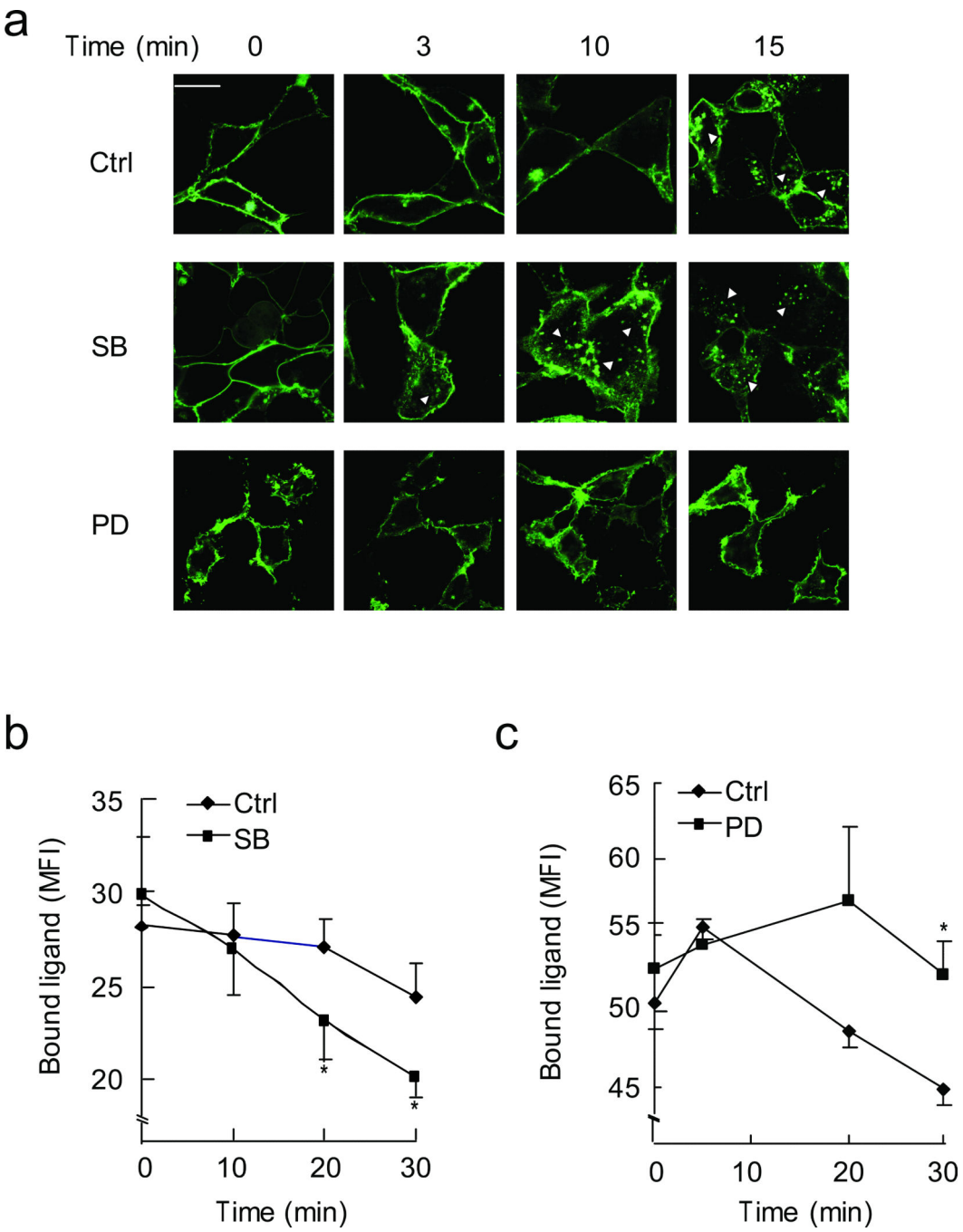

Figure 5. p38 MAPK and Erk differentially regulate FPR1 internalization

(**a**) fMLP (100 nM) induced internalization of FPR1-YFP in control (Ctrl), SB203580 (SB, 10 μM), and PD98059 (PD, 50 μM)-treated HEK293 cells at indicated times. Arrowheads point to the internalized receptor. Three independent experiments were performed, each using > 30 cells per condition. Bar, 20 μm. (**b, c**) Internalization of FPR1 in HL60 cells in the presence and absence of SB203580, 10 μM (**b**), or PD98059, 50 μM (**c**). *, $P < 0.05$, compared to control. Results are mean of 3 independent experiments; 2×10^5 cells were used for each condition. Bars indicate mean ± SEM.

Author Manuscript Author Manuscript Author Manuscript Author Manuscript

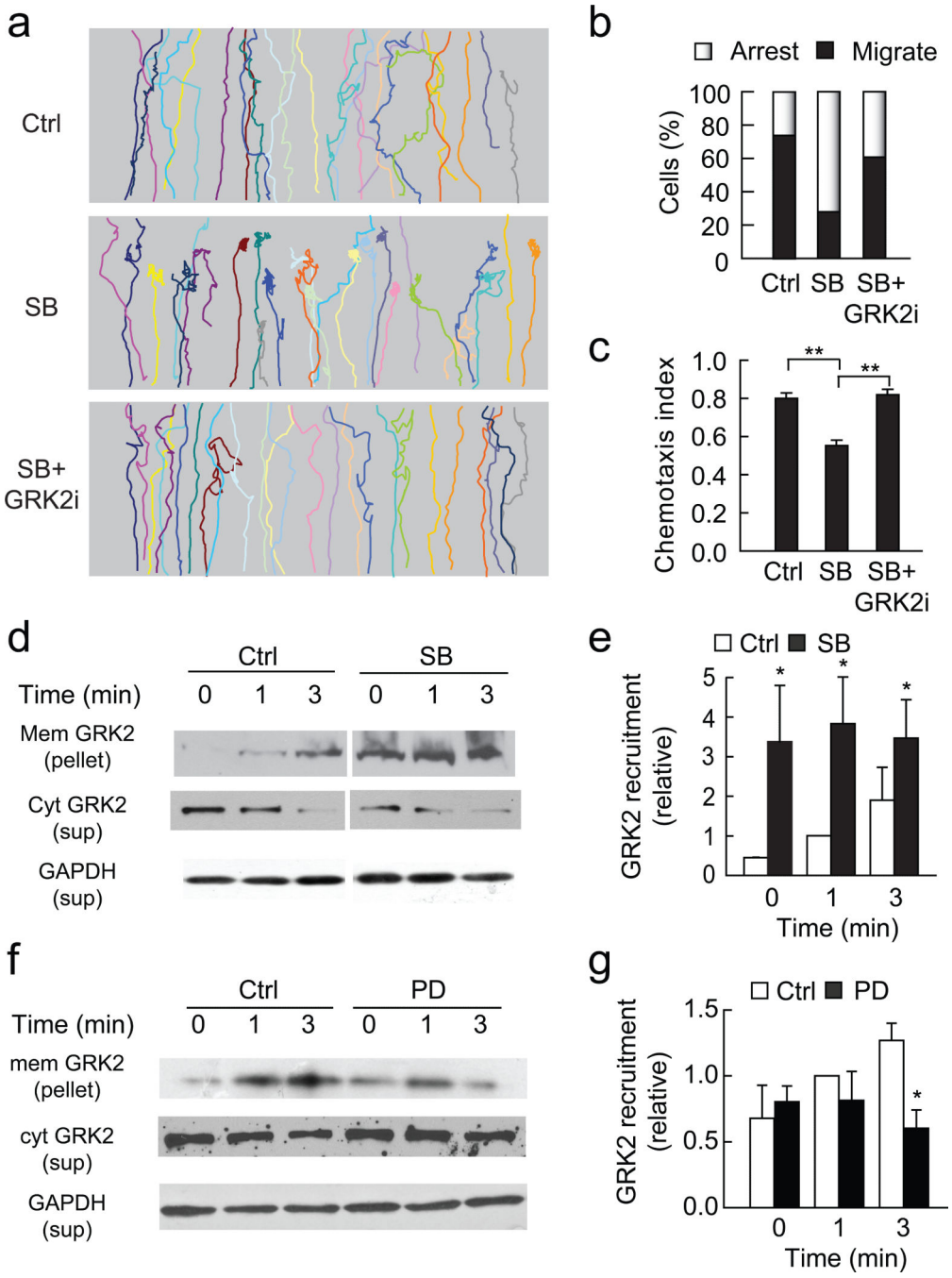

Figure 6. GRK2 mediates the "stop" signal for neutrophil migration

(**a**) Trajectories of control (ctrl), SB203580-treated (SB), SB203580-treated GRK2 RNAi cells (SB+GRK2i), in 100 nM fMLP gradient. Three independent experiments were performed, each using > 30 cells per condition, one of representative experiments is shown. (**b**) Relative percentage of cells migrated through (black bars) and arrested (open bars) in above three groups of cells. (**c**) CI of above three groups of cells. *, $P < 0.001$. Results are mean of 3 independent experiments; bars indicate mean ± SEM. (**d, e**) Immunoblots of membrane (mem) and cytosol (cyt) GRK2 in the presence and absence of SB; sup,

Author Manuscript Author Manuscript Author Manuscript Author Manuscript

supernatant. (**f, g**) Immunoblots of membrane and cytosol GRK2 in the presence and absence of PD. Values were compared with that of non-treated cells (Ctrl) at 1 min (as 1). **, $P < 0.05$, compared to control. $N = 3$, one of representative experiments is shown.

Author Manuscript Author Manuscript Author Manuscript Author Manuscript

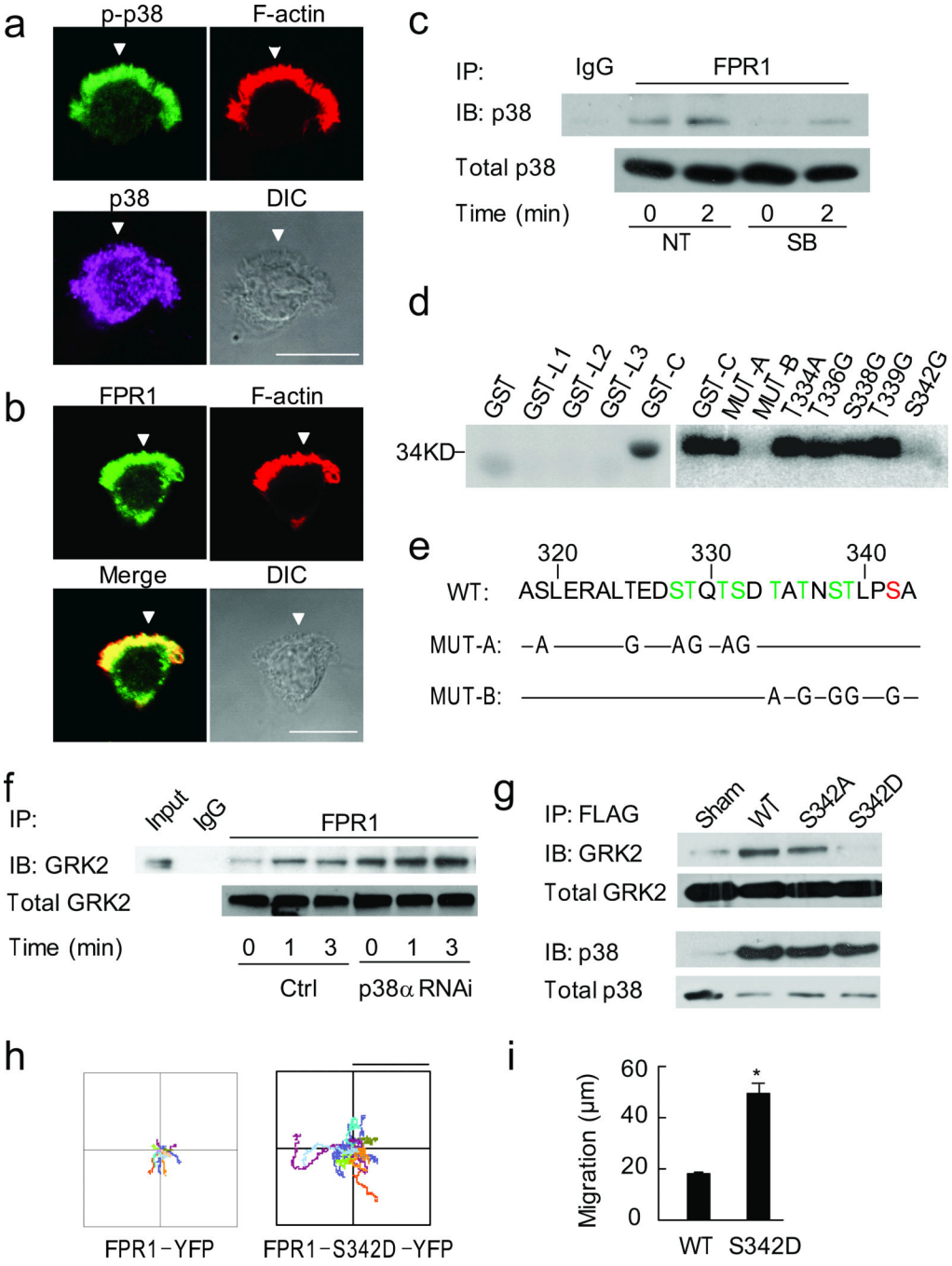

Figure 7. p38 MAPK phosphorylates FPR1

(**a, b**) Immunostaining of p-p38, p38 (**a**) and FPR1 (**b**) in HL60 cells. Bar, 10 μm. Arrowheads point to pseudopods. $N > 30$ cells. (**c**) Immunoprecipitation between FPR1 and p38, one of 3 separated experiments is shown. (**d**) Autoradiograph of ^{32}P-labeled peptides. L1-3 and C, loop1-3 domains and c-terminal of FPR1; MUT-A, Ser/Thr residues within 319-332 were mutated to Ala/Gly; MUT-B, Ser/Thr residues within 334-342 were mutated to Ala/Gly, also see panel **e**. $N = 3$. (**e**) Wild-type and mutants of the 11 Ser/Thr residues in the c-terminal of FPR1. Phosphorylation sites by GRK2 (green) and p38 MAPK (red). (**f**)

Author Manuscript Author Manuscript Author Manuscript Author Manuscript

Immunoprecipitation between FPR and GRK2 in control and p38α RNAi cells, $n = 3$; *, $P < 0.05$, compared to control. (**g**) Immunoprecipitation of WT and mutant FPR1 (S342A and S342D) with GRK2 and p38 MAPK, one of 3 separated experiments is shown. *, $P < 0.05$, compared to WT. (**h**) Trajectories of FPR1-YFP and FPR1-S342D-YFP expressing cells stimulated with fMLP (500 nM). $N = 3$, each using > 30 cells per condition. Bar, 60 μm. (**i**) Distance migrated of above two groups of cells. *, $P < 0.001$. Bars indicate mean ± SEM.

Author Manuscript Author Manuscript Author Manuscript Author Manuscript

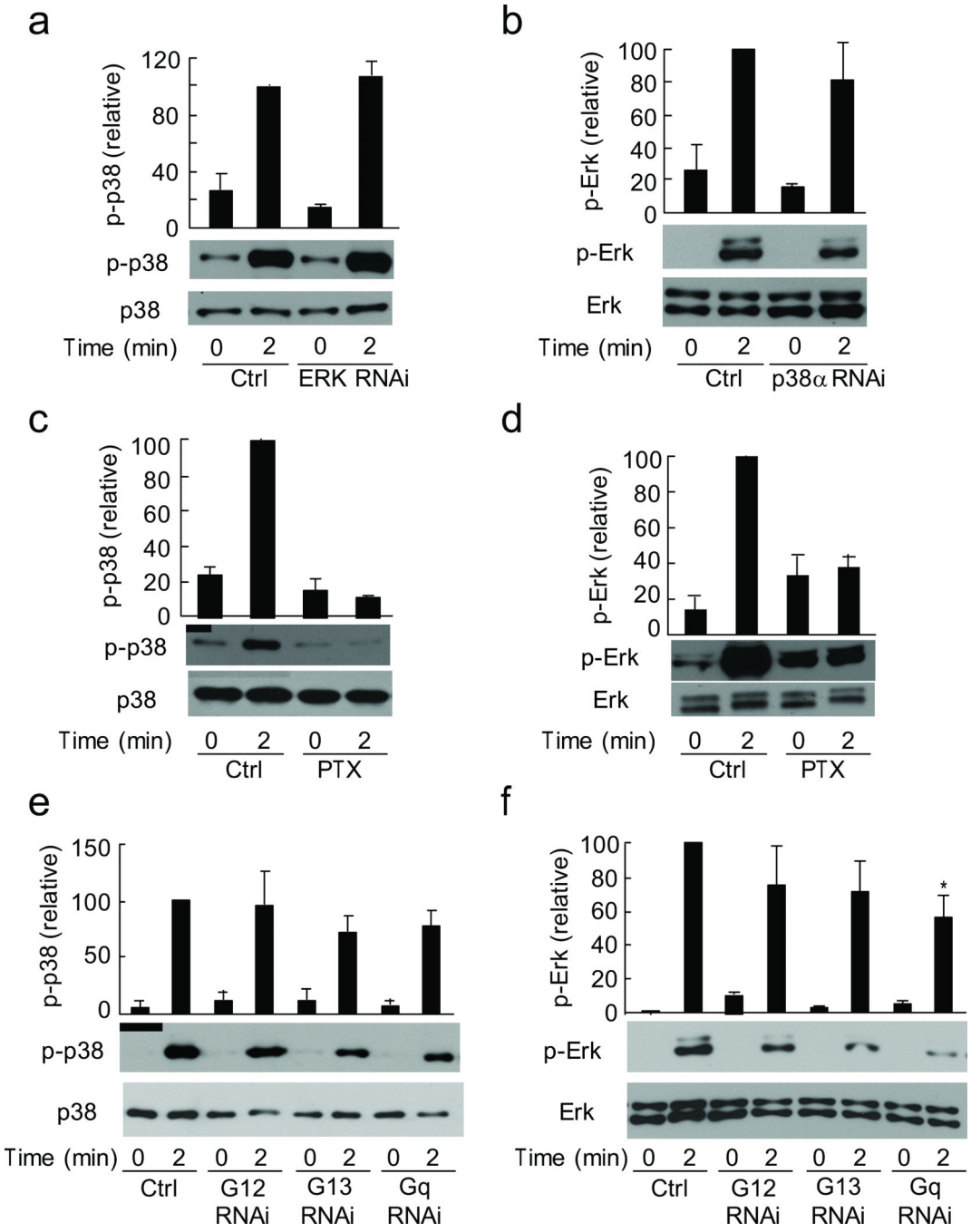

Figure 8. Differential activation of Erk and p38 MAPK

(**a, b**) Immunoblots show p-p38, p38 (**a**), p-Erk and Erk (**b**) in control, p38 RNAi or Erk RNAi cells (100 nM fMLP). p-p38 and p-Erk values were compared to control at 2 min (as 100). One of 3 separated experiments is shown; bars indicate mean ± SEM. (**c, d**) Immunoblots show p-p38, p38 (**c**), p-Erk and Erk (**d**) in control and PTX (1 μg/ml) treated cells. p-p38 and p-Erk values were compared to control at 2 min (as 100). *N* = 3, one of representative experiments is shown; bars indicate mean ± SEM. (**e, f**) Immunoblots show p-p38, p38 (**e**), p-Erk and Erk (**f**) in control, G12, G13, or Gq RNAi cells. p-p38 and p-Erk

values were compared to control at 2 min (as 100). $N = 3$, one of representative experiments is shown; *, $P < 0.05$, compared to control. Bars indicate mean ± SEM.

Author Manuscript Author Manuscript Author Manuscript Author Manuscript